Creation of a Control Dataset and Forecast System for Global Observing System Simulation Experiments (OSSEs)*

Sean P.F. Casey[1†], Robert Atlas[2], Ross N. Hoffman[1], Lidia Cucurull[2,3], John S. Woollen[4], Isaac Moradi[5], Narges Shahroudi[6], Sid-Ahmed Boukabara[6], Kayo Ide[7], Ruifang Li[3], Nikki Privé[8], and Fanglin Yang[4]

[1]*University of Miami/Cooperative Institute for Marine and Atmospheric Sciences (CIMAS) and National Oceanic and Atmospheric Administration (NOAA)/Atlantic Oceanic and Meteorological Laboratory (AOML)/Hurricane Research Division (HRD), Miami, FL*

[2]*NOAA/AOML, Miami, FL*

[3]*NOAA/Earth System Research Laboratory (ESRL), Boulder, CO*

[4]*NOAA/National Centers for Environmental Prediction (NCEP)/Environmental Modeling Center (EMC), College Park, MD*

[5]*National Aeronautics and Space Administration (NASA)/Goddard Space Flight Center (GSFC), Greenbelt, MD*

[6]*NOAA/National Environmental Satellite, Data, and Information Service (NESDIS)/Center for Satellite Applications and Research (STAR), College Park, MD*

[7]*University of Maryland, College Park, MD*

[8]*Morgan State University, Baltimore, MD*

Motivation

Every 6 hours, roughly 4 million observations are assimilated into the operational NCEP/Global Forecast System (GFS) model, using Gridpoint Statistical Interpolation (GSI). When conducting OSSEs, we cannot assess the global impacts of potential new observing systems without first creating a control dataset, mirroring these roughly 4 million observations. This globally-simulated control dataset should (a) use geolocation similar to that in the real world, (b) have similar error characteristics as the real-world observations, and (c) yield similar forecast skill to control observations in the real world. This extended abstract describes the methods used to create such a dataset for use in global OSSEs conducted with GFS and simulated from the NASA Goddard Earth Observing System Model, Version 5 (GEOS-5) 7-km Nature Run (G5NR).

Observations

The simulation of observations was covered extensively in Boukabara et al. (2016), and will be briefly summarized here. The experiment period chosen for this study was August/September 2006 of the G5NR simulated atmosphere. In order for our global OSSE results to better reflect potential impacts in

* Extended abstract for the poster presentation of Casey et al. (2017b).

† Sean.Casey@noaa.gov

the current observational system, we must use a more complete and recent observation system (here chosen to be 2014), rather than observations available in 2006. Locations for August/September 2014 were used to simulate observations from August/September 2006 in the G5NR. Table 1 lists the control observation sources simulated from 2014 observations; this includes all control observation types except for tropical cyclone (TC) minimum surface pressure.

Storms are detected and tracked in the G5NR in two stages. The first stage is automated: a TC is detected if the values of central pressure, maximum 10 m wind speed, maximum vorticity, and temperature difference between the storm core and surroundings exceed fairly stringent thresholds [Putman (2015), Reale et al. (2017)]. G5NR storm tracks for 2005 and 2006 in several ocean basins are plotted in the figures of Chapter 4 of Gelaro et al. (2014). The thresholds and specifications of the levels for maximum vorticity and presence of a warm core were tuned to eliminate shallow storms that did not fully develop. For example, in the presence of strong shear it is unlikely that a warm core will be present at high levels. All storm fixes of central pressure, location and storm motion, detected in this way in the entire G5NR were converted to TCVitals format.

While the automated stringent storm detection is successful at eliminating circulations that are not quite TCs, it misses the genesis and lysis of the detected TCs. Figure 1 shows one such TC, which would be considered a Category 1 Hurricane by the National Hurricane Center (NHC) that is completely missed by the Putman/Reale criteria; it was discovered during manual inspection of TC lifecycles within the G5NR. To capture the full life cycle of the storms detected in the first stage, we extended the TCVitals records for these storms in a less stringent second stage that searches forward and backwards in time to add occurrences of minimum surface pressure less than 1005 hPa and maximum 10 m wind speed greater than 18 m s^{-1}, provided there is no land within the 2°×2° latitude-longitude box centered on the location of the minimum surface pressure

Added Errors

GSI calculates observation innovation [or, observation minus background (O-B)] for each observation type, with additional separation for vertical height (for conventional and GPSRO observations) and by channel (for radiances). For most observation types the observation innovation will show significant differences between real and simulated "perfect" (i.e., no error added) observations. Figure 2 shows the bias and RMSE added to IASI/Metop-B simulated radiances (clear sky) in order to better match error characteristics noted in real observations. The error statistics used were determined using a method similar to Errico et al. (2013). The same approach is applied for all observation types, with the exception of tropical cyclones.

The general approach of tuning observational errors by matching innovations in reality and the OSSE is not applicable in the case of TCVitals. First, the global sample is small, and should be divided into even smaller samples since the errors are known to depend strongly on at least two factors—storm intensity and whether aircraft observations are available. Second, most of the intensity innovation comes from the background. The background may have location errors, and the background intensity errors are inhomogeneous, becoming larger and more biased as the TC gets more intense and smaller scale.

Adding errors to the observation will not make up for deficiencies in the background. Third, vortex relocation statistics would have to be matched also. As a result, we rely on published estimates of TCVitals records.

Previous studies show that TCVitals and best track uncertainty depends on intensity and whether or not aircraft observations were available. Previous studies include comparisons of TCVitals and best track (Trahan and Sparling 2012), estimates of TCVitals errors (Torn and Snyder 2012), and estimates of best track errors (Landsea and Franklin 2013). As expected, uncertainties for intensity and track are smaller when aircraft observations are available. As intensity increases, intensity uncertainty increases and position uncertainty decreases. As a result our estimates of simulated errors are stratified by intensity and availability of aircraft observations. As a proxy, we assume aircraft observations are available for all fixes west of 60W in the Atlantic and Caribbean (Torn and Snyder 2012, Fig. 4).

TCVitals simulated observations are assumed to have zero mean Gaussian errors in central pressure and eastward and northward displacements. We simulate the errors in central pressure and eastward and northward displace3ments as $\delta p_c = \sigma_p q$, $\delta x = \sigma_d u$, and $\delta y = \sigma_d dv$, where q, u, and v are sampled from a standard normal distribution. The standard deviations, σ_p and σ_d are based on Table 2 of Landsea and Franklin (2013) and are presented in Table 2 in terms of standard deviation for three different classes of storms and for two regions—the western Atlantic and everywhere else.

The values reported by Landsea and Franklin (2013) are subjective uncertainty estimates of best tracks. TCVital errors are expected to be somewhat larger than best track errors. That said, we take the best track uncertainty estimates of Landsea and Franklin (2013) as estimates of the TCVitals uncertainty. First, Landsea and Franklin (2013) is the only study that provides estimates for different intensity and observing system categories. Second, with increasing access to observations in real time, the accuracy of future TCVitals may equal or exceed that of present best tracks. For example, Fig. 11 of Torn and Snyder (2012) shows improvement in the accuracy of TCVitals track positions over time. Third, TCVitals and best track uncertainty estimates are themselves uncertain. Finally, the application of subjective uncertainty measures is open to interpretation.

With respect to this last point, "mean absolute error may be the best way to consider" Table 2 of Landsea and Franklin (2013), according to C. Landsea (pers. Comm.., July 9, 2015). To convert mean absolute error (MAE) to standard deviation (STD) note that

$$|\delta p_c| = \sigma_p |q| = \sigma_p (q^2)^{1/2}$$

is σ_p times a χ-random variable with one degree of freedom (*dof*) and that

$$\delta r = (\delta x^2 + \delta y^2)^{1/2} = \sigma_d (u^2 + v^2)^{1/2}$$

is σ_d times a χ-random variable with two *dof*. Thus, with $\langle . \rangle$ denoting expectation, the relationships between MAE and STD are given by

$$MAE(\delta p_c) = \langle |\delta p_c| \rangle = \sigma_p \langle \chi_1 \rangle = \sigma_p \sqrt{\frac{2}{\pi}}$$

$$MAE(\delta r) = \langle \delta r \rangle = \sigma_d \langle \chi_2 \rangle = \sigma_d \sqrt{\frac{\pi}{2}}$$

In our implementation, we use the fact that δr^2 is σ_d^2 times a χ_2^2 random variable and that heading direction for the position error is 2π times a [0, 1] uniform random variable.

Model Configurations

The National Weather Service (NWS)/NCEP GFS is used for OSSE experiments. An operational version utilized in 2015 (NWPROD_2015_Q1) is the starting point for the OSSE system set-up. While the operational version ran at T1534, a lower-resolution research version is used here. This version is used to run the 7-day Global Spectral Model (GSM) forecasts at T670 spectral truncation, with hybrid GSI-based three-dimensional ensemble-variation (3DEnVar) run at T254.

Two changes were made to the NWPROD_2015_Q1 setup in order to work within the Global OSSE system. First, the spatial-averaging steps in read_atms.f90 and read_ssmis.f90 (in GSI) were commented out; while this is necessary for real observations due to different footprint sizes and locations, the OSSE data simulation uses the same geolocation for every channel, rendering this step unnecessary.*

The second change regarded GSM configuration-file parameters. Without changes to these parameters, the forecast skill for the OSSE was found to be much higher than that for the real world; this suggests a "fraternal-twin" scenario between the GEOS-5 model physics and the GFS physics, where GFS is better able to predict what GEOS-5 will do than the atmosphere in the real world. In consultation with Fanglin Yang of EMC, it was decided to increase two configuration-file parameters, with the goal of degrading the GSM forecasts. To accomplish this, the mountain block and orographic drag coefficients (cdmbgwd) are doubled from '0.75, 3.00' to '1.50, 6.00', and the vertical momentum diffusion coefficient (bkgd_vdif_m) is doubled from 3.00 to 6.00. Tests showed this reduced the forecast skill, better approximating real-world conditions in the OSSE system.

Test Observations

With the control dataset simulated, with explicit observation errors added, and with the model configuration set, we can now begin the process of simulating prospective new observations and running forecasts to test these. For example, Figure 3 shows simulated 12.8-micron observations for five Geostationary Hyper-Spectral Sounders (GeoHSS), located at 0°E, 60°E, 140°E, 225°E, and 285°E longitude. Experiments testing the impact of these simulated new observations were discussed in Casey et al. (2017a).

* Running GSI without these steps commented out, however, and assimilating OSSE observations will result in a system crash.

References

Boukabara, S.-A., I. Moradi, R. Atlas, S. P. F. Casey, L. Cucurull, R. N. Hoffman, K. Ide, V. K. Kumar, R. Li, Z. Li, M. Masutani, N. Shahroudi, J. Woollen, and Y. Zhou, 2016: Community Global OSSE Package (CGOP): Description and Usage. *J. Atmos. Oceanic Technol.*, **33**, 1759-1777, doi:10.1175/JTECH-D-16-0012.1.

Casey, S. P. F., R. Atlas, R. N. Hoffman, L. Cucurull, and N. Shahroudi, 2017a: Global OSSEs for Error-Added Geo-Hyper IR (IASI) Observations. *21st Conference on Integrated Observing and Assimilation Systems for the Atmosphere, Oceans, and Land Surface. American Meteorological Society 97th Annual Meeting,* Seattle, WA, January 2017. https://ams.confex.com/ams/97Annual/webprogram/Paper307087.html.

Casey, S. P. F., R. Atlas, R. N. Hoffman, L. Cucurull, J. S. Woollen, I. Moradi, N. Shahroudi, S. A. Boukabara, K. Ide, R. Li, N. Privé, and F. Yang, 2017b: Creation of a Control Dataset and Forecast System for Global OSSEs. *21st Conference on Integrated Observing and Assimilation Systems for the Atmosphere, Oceans, and Land Surface. American Meteorological Society 97th Annual Meeting,* Seattle, WA, January 2017. https://ams.confex.com/ams/97Annual/webprogram/Paper307082.html.

Errico, R. M., R. Yang, N. C. Privé, K.-S. Tai, R. Todling, M. E. Sienkiewicz, and J. Guo, 2013: Development and validation of observing-system simulation experiments at NASA's Global Modeling and Assimilation Office. *Quart. J. Roy. Meteor. Soc.*, **139**, 1162-1178, doi:10.1002/qj.2027.

Gelaro, R., and Coauthors, 2014: Evaluation of the 7-km GEOS-5 nature run. *Technical Report Series on Global Modeling and Data Assimilation*, R. D. Koster, Ed., NASA, Greenbelt, MD, Goddard Space Flight Center, Vol. 36, 305 pp. TM-2014-104606v36.

Landsea, C. W., and J. L. Franklin, 2013: Atlantic hurricane database uncertainty and presentation of a new database format. *Mon. Wea. Rev.*, **141**(10), 3576-3592, doi:10.1175/mwr-d-12-00254.1.

Putman, W. M., 2015: Overview. Evaluation of the 7-km GEOS-5 nature run, R. D. Koster, Ed., NASA/TM-2014-104606, Tech. Rep. Series on Global Modeling and Data Assimilation, Vol. 36, 1-29.

Reale, O., D. Achuthavarier, M. Fuentes, W. Putman, and G. Partyka, 2017: Tropical Cyclones in the 7-km NASA Global Nature Run for Use in Observing System Simulation Experiments. *J. Atmos. Oceanic Technol.*, **34**, 73-100, doi:10.1175/JTECH-D-16-0094.1.

Torn, R. D., and C. Snyder, 2012: Uncertainty of tropical cyclone best-track information. *Wea. Forecasting*, **27(3)**, 715-729, doi:10.1175/waf-d-11-00085.1.

Trahan, S., and L. Sparling, 2012: An analysis of NCEP tropical cyclone vitals and potential effects on forecasting models. *Wea. Forecasting*, **27 (3)**, 744-756, doi:10.1175/waf-d-11-00063.1.

- **Surface Pressure Types (IDs)**
  - Rawinsonde (120)
  - Dropsonde (132, 182)
  - Surface Marine (180)
  - Surface Land (181)
  - Surface METAR (187)
- **Conventional Wind Types (IDs)**
  - Rawinsonde (220)
  - PIBAL (221)
  - NPN Wind Profiler (223)
  - NEXRAD (224)
  - Wind Profiler – PIBAL Decoded (229)
  - Aircraft (230, 231, 233)
  - Dropsonde (232)
  - Surface Marine (280)
- **Moisture Types (IDs)**
  - Rawinsonde (120)
  - Dropsonde (132, 182)
  - Surface Marine (180)
- **Satellite Wind Sources (IDs)**
  - JMA (242, 250, 252)
  - EUMETSAT (Meteo-Sat) (243, 253)
  - NESDIS-GOES (245, 246)
  - MODIS/POES (Aqua) (257, 258, 259)
  - ASCAT (290)
- **Temperature Types (IDs)**
  - Radiosonde (120)
  - Aircraft (130, 131, 133)
  - Dropsonde (132, 182)
  - Surface Marine (180)
- **Radiance Instruments (Satellites)**
  - Aqua (AIRS, AMSU-A)
  - F17 (SSMIS)
  - F18 (SSMIS)
  - GOES 15 [GOES Sounder (4 detectors)]
  - M10 (SEVIRI)
  - Metop-A (AMSU-A, HIRS4, IASI, MHS)
  - Metop-B (AMSU-A, IASI, MHS)
  - N15 (AMSU-A)
  - N18 (AMSU-A, MHS)
  - N19 (AMSU-A, MHS)
  - NPP (ATMS/CrIS)
- **GPS Bending Angle (IDs)**
  - Metop-B (003)
  - Metop-A (004)
  - TSX (042)
  - COSMIC (740-745)

Table 1: List of all simulated control observations (except for tropical cyclone surface pressure). Observation locations from August/September 2014 are used to simulate observations from August/September 2006 in the G5NR.

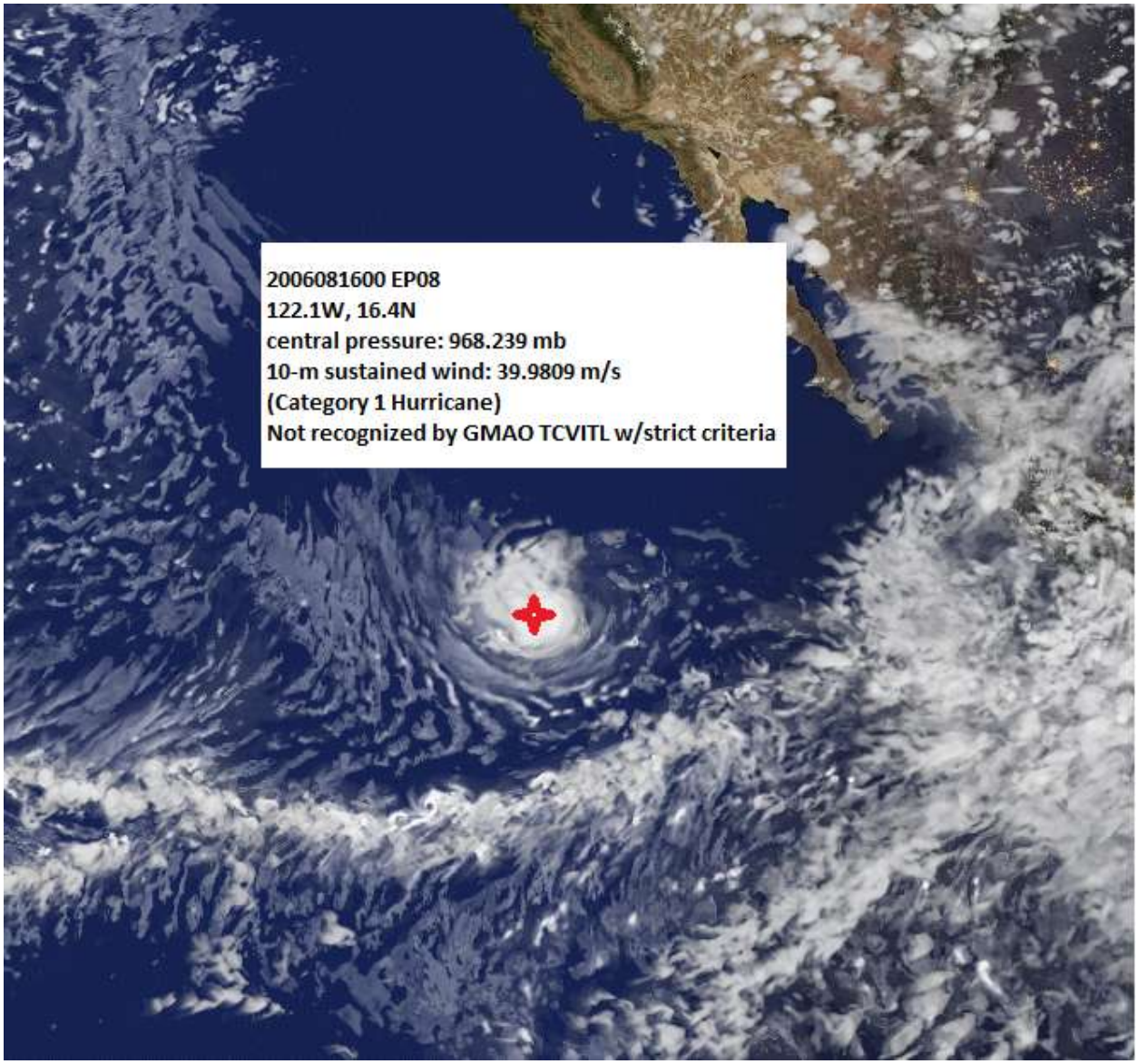

Figure 1: Tropical Cyclone EP08, as it appears in the G5NR on 2006081600. EP08 was not recognized as a tropical cyclone at this time by the Putman/Reale algorithm.

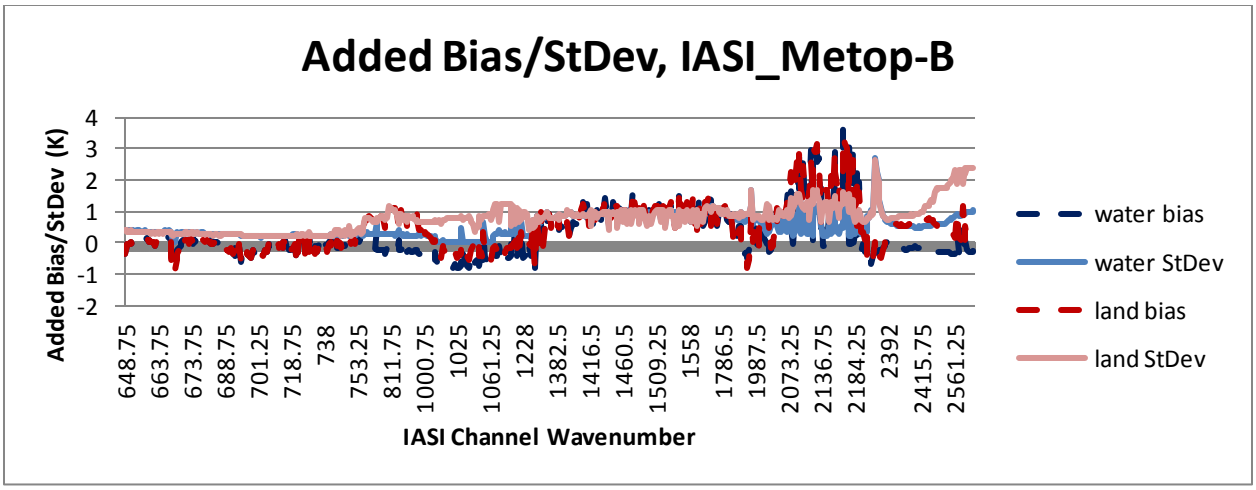

Figure 2: Explicit observation error added to IASI/Metop-B channels, separately by surface (water/land).

Basin/Metric	Tropical Storms	Category 1-2	Category 3-5
Atlantic west of 60°			
-pressure (mb)	3.8	4.4	4.9
-location (n mi)	27.5	18.6	14.0
All others			
-pressure (mb)	7.3	9.6	11.9
-location (n mi)	43.1	29.0	15.4

Table 2: Explicit observation error added to tropical cyclone observations (pressure and location), based on location of TC center.

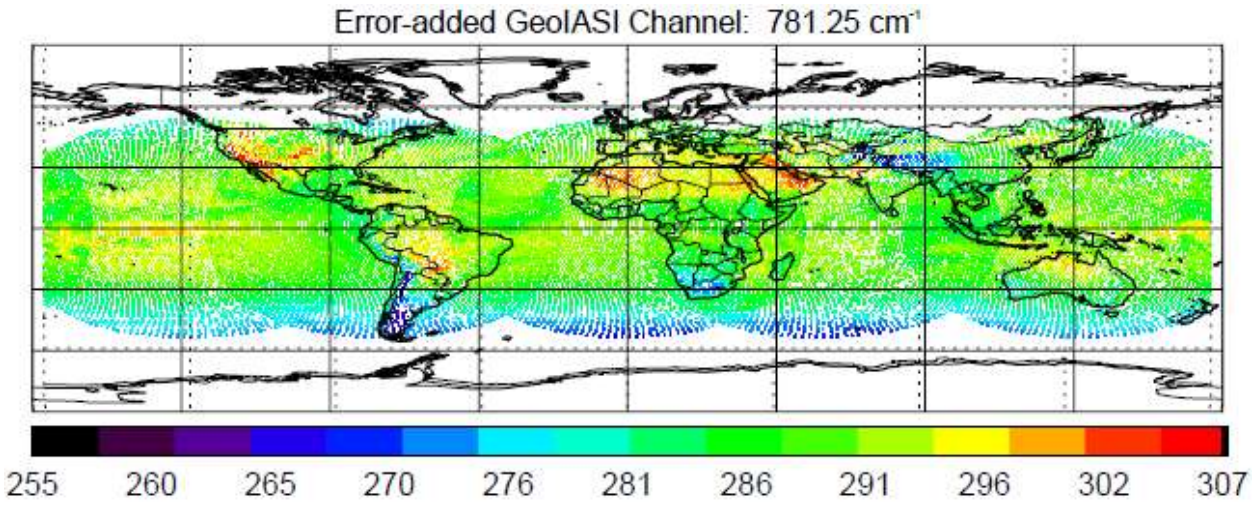

Figure 3: Simulated clear sky 12.8-micron observations from five Geostationary Hyper-Spectral Sounder (GeoHSS) satellites seated at 0°E, 60°E, 140°E, 225°E, and 285°E on 2006081500 (G5NR).